Complex motion of precipitation bands

István Lagzi [a,*], Péter Pápai [b], Zoltán Rácz [b]

[a] *Institute of Chemistry, Eötvös University, 1117 Budapest, Pázmány sétány 1/a, Hungary*
[b] *Institute for Theoretical Physics – HAS, Eötvös University, 1117 Budapest, Pázmány sétány 1/a, Hungary*

Abstract

Formation and dynamics of an $Al(OH)_3$ precipitation ring is studied by diffusing NaOH into a gel containing $AlCl_3$. Limited feeding of the outer electrolyte (NaOH) is found to yield an intricate ring-dynamics which involves stopping and reversal of the direction of motion of the precipitation ring, and evolution into stationary multi-ring structures. A model of the ring-dynamics is developed by combining a phase separation scenario for the precipitation with the redissolution (complex formation) of the precipitate in the excess of the outer electrolyte.
© 2006 Elsevier B.V. All rights reserved.

1. Introduction

Precipitation patterns formed in the wake of moving reaction fronts have been studied for a long time [1]. Recent interest in these structures stems from possible relevance to engineering mesoscopic and microscopic patterns [2–6]. In contrast to removing material to construct a structure (top–down processing), controlled precipitation is suggested as means to generate a prescribed bulk design (bottom–up processing). In order to understand how to guide and locate precipitation regions, it is instrumental to investigate cases where, in addition to precipitation in the reaction zone, redissolution in the wake of the moving front also takes place [7–15]. The resulting virtual motion of a precipitation pulse (or more complicated pattern) is easily visualized and its dynamics can be studied in detail.

In a usual setup for observing moving precipitation pulses, the inner electrolyte is distributed homogeneously in a gel column and the outer electrolyte diffuses into this medium (typical examples of inner/outer electrolyte pairs are Hg^{2+}/I^-, Co^{2+}/NH_4OH, Cr^{3+}/OH^-). The precipitate (HgI_2, $Co(OH)_2$, $Cr(OH)_3$) forms in the reaction zone which moves diffusively along the column. In the wake of this front, the excess of the outer electrolyte consumes the precipitate and forms a complex ($[HgI_4]^{2-}$, $[Co(NH_3)_6]^{2+}$, $[Cr(OH)_4]^-$). In cases when the gel, the reagents, and the complex are transparent, while the precipitate is not, the position of the precipitation pulse (band) is easily monitored.

Our aim here is to study the dynamics of precipitation pulses in radially symmetric, two-dimensional setup with limited feeding of the outer electrolyte. From experimental side, we present a quantitative description of the radial motion of precipitation pulses with emphasis on the stopping of the band and on the reversal of the radial motion with the ensuing multiplication of the precipitation bands. From theoretical side, we generalize the so-called phase separation theory of Liesegang phenomena [17], and show that the novel aspects of the experiments (reversal of front motion and the multiplication of bands) can be described well but problems arise when such detail as the time-evolution of the width of the precipitation band is considered.

2. Experiments

The evolution of the precipitation pulse is observed in the following reaction scheme [14]:

$$Al^{3+}(aq) + 3OH^-(aq) \rightarrow Al(OH)_3(s)$$
$$Al(OH)_3(s) + OH^-(aq) \rightarrow [Al(OH)_4]^-(aq).$$

---
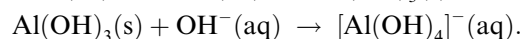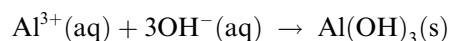
* Corresponding author.
  E-mail address: lagzi@vuk.chem.elte.hu (I. Lagzi).

Agarose (Reanal) was dissolved in distilled water to produce 1% solution. It was continuously stirred and heated up to 90 °C. The clear solution was mixed with the given amount of $AlCl_3 \cdot 6H_2O$ (Reanal), and this solution was poured into a Petri dish to obtain a uniformly thick gel (3.2 mm). After polymerization, a circular hole of radius R is cut out at the center of the gel, and the outer electrolyte of fixed concentration ($a_0 = 2.50$ M) was placed into this reservoir. No feeding of the outer electrolyte (usual boundary conditions in many experiments and simulations) was allowed. The parameters varied in the experiments were the concentration of the inner electrolyte (b_0) and the radius of the reservoir (R). When changing R, the volume V_0 of the outer electrolyte was changed proportionally to R^2.

Shortly after the outer electrolyte is placed into the reservoir, a white precipitate can be observed at the gel-reservoir interface. Next, the thin precipitation ring detaches from the interface (due to redissolution of the precipitate in the wake of the outward moving reaction front). The precipitation band is well visible because both the aluminum chloride and its hydroxo complex are colorless in contrast to the white precipitate, $Al(OH)_3$. At early stages, the increase of radius of the pulse $r_f(t)$ is proportional to the square root of time $r_f(t) - R \sim \sqrt{t}$, indicating that the front motion is driven by diffusion of the invading electrolyte. Then the front motion slows down (faster than in case of continuous feeding) and, finally, the front stops (Fig. 1a). The total increase in the radius $r_f(\infty) - R$ depends on the concentrations of the inner- and outer-electrolytes, and on radius of the reservoir. The value of $r_f(\infty) - R$ can be easily estimated from the mass conservation law.

The width $w(t)$ of the pulse shows a more complicated behavior (Fig. 1b). It increases up to a maximum value and, as the front significantly slows, it starts to decrease. In this regime, the precipitation stops at the outer edge of the pattern, the reason being that the limited feeding cannot maintain the necessary concentration for the formation of the precipitate. Nevertheless, even the limited feeding is sufficient for the complex formation in the wake of the front, and w decreases. Similar sequence of events can be observed at fixed R (fixed amount of the outer electrolyte) when varying the concentration of the inner electrolyte (Fig. 2). The effect of concentration of the electrolytes on front velocity has been studied in previously [7,12], and it was found that the velocity of pattern formation is higher at lower concentration of the inner electrolyte. Here we find that lowering of concentration of the inner electrolyte mainly affects the temporal evolution of the width. Namely, for very low concentrations, $w(t) \sim \sqrt{t}$ behavior can be seen all the way to the time when the pulse stops. We do not have an explanation for this. The observation that the concentration of the precipitate visibly decreases at the outer edge of the front, however, suggests that a colloidal retransformation of the precipitation ring compensates the complex formation which would otherwise decrease the width.
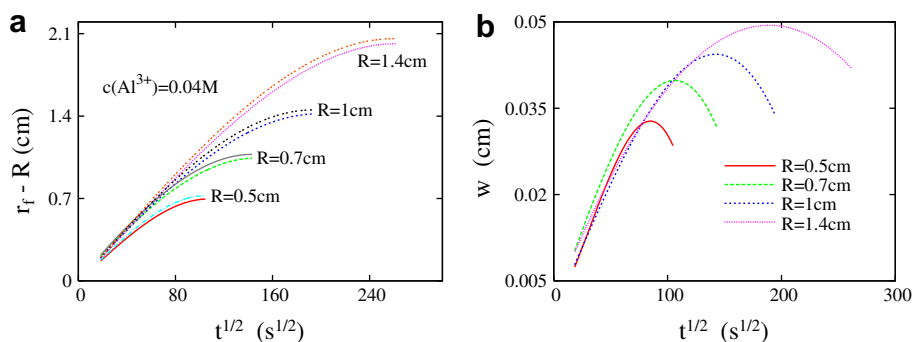

Fig. 1. Radius (a) and width (b) of the precipitation ring plotted as a function of $\sqrt{t}$ with time measured in seconds. The position of both the leading edge and the back of the ring are plotted on (a) for various radii (R) of the reservoir where the outer electrolyte is confined initially.
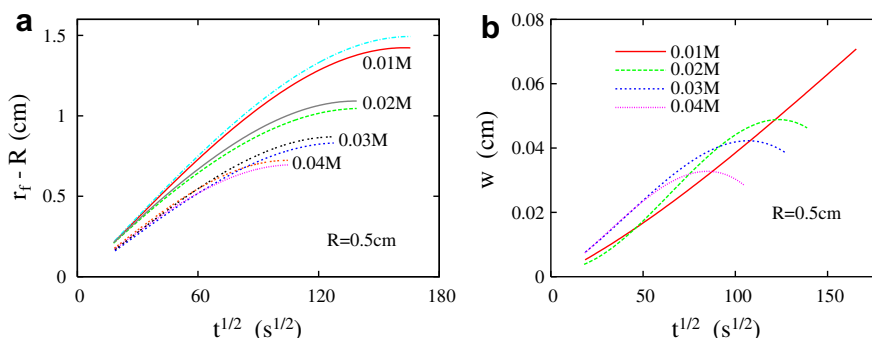

Fig. 2. The same as in Fig. 1a and b but for various initial concentration of the inner electrolyte. The radius of the container where the outer electrolyte is initially confined is also kept constant ($R = 0.5$ cm).
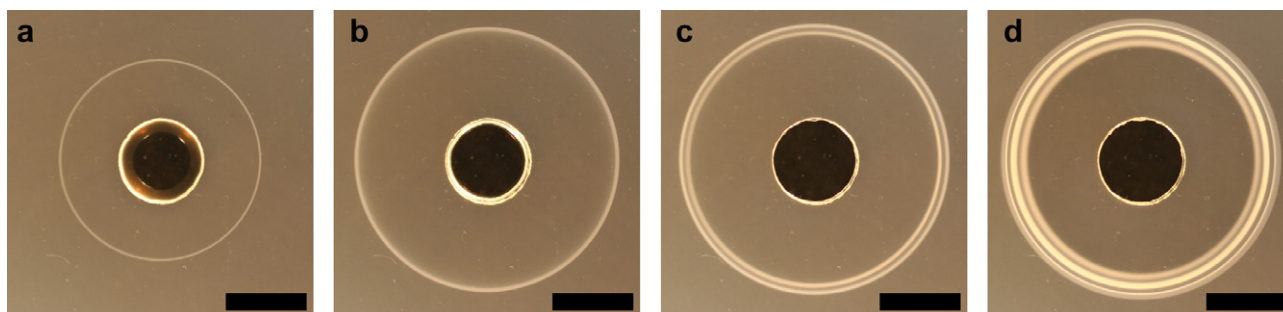
Fig. 3. Evolution of the precipitation pulse ($[AlCl_3]_0 = 0.02$ M, $[NaOH]_0 = 2.50$ M, $V_0 = 125$ μL, and $R = 0.5$ cm): (a) single ring at $t = 1$ h; (b) band stops ($t = 1.5$ h); (c) new ring forms inside the outer ring ($t = 5$ h); (d) triple ringed structure ($t = 6.5$ h). The scale bar is 1 cm.

An interesting phenomenon can be observed after the precipitation pulse stops. As shown in Fig. 3, a new well-separated ring emerges inside the stationary pulse. It appears that the precipitation front reverses its motion (reversal of reaction front motion for specially prepared initial conditions have been seen previously [16]). Supporting the picture of the reversal of the front is that a third ring with even smaller radius forms after a while and, furthermore, the outer rings do not get dissolved. This means that the outer electrolyte is confined to regions with radius smaller than that of the stationary rings.

3. The model and the simulation results

In order to model the phenomena described in Section 2, let us first note that the reactions take place in a gel. Thus, no convection is present, and the primary dynamics is a slow reaction–diffusion process. Denoting the reagents of the outer- and inner-electrolytes by $A \equiv OH^-$ and $B \equiv Al^{3+}$, respectively, the first stage of the process, $3A + B \rightarrow C$, yields a reaction product $C \equiv Al(OH)_3$. The next step is the formation of precipitate which will be modeled as phase separation of C into low- and high-concentration regions of C as described by the Cahn–Hilliard equation. A similar strategy has been successfully employed in the theory of Liesegang phenomena [17,18] where the above two steps constitute the whole pattern formation process. The new element here is that the outer electrolyte forms a complex with the precipitate ($A + C \rightarrow D \equiv [Al(OH)_4]^-$). The complex formation is responsible for the redissolution of C and, consequently, for the moving precipitation band. For simplicity, we shall assume that, once the complex is formed, it ceases to play any active role in the reactions. This assumption appears to be justified in the given experiment.

Denoting the concentrations of A, B, and C by a, b, and c, respectively, the above understanding (model) is described by the following equations

$$\partial_t a = D_a \Delta a - 3ka^3 b - ga(c - c_1) \tag{1}$$

$$\partial_t b = D_b \Delta b - ka^3 b \tag{2}$$

$$\partial_t c = -\lambda \Delta \frac{\delta f}{\delta c} + ka^3 b - ga(c - c_1). \tag{3}$$

Here D_a, D_b are the diffusion coefficient of A and B, respectively, k and g are the reaction rate constants, λ is the kinetic coefficient giving the timescale of the phase separation process. The phase separation is governed by a free energy functional $f(c)$ with two minima in homogeneous states corresponding to the equilibrium high- (c_h) and low- ($c_1 \approx 0$) concentrations of C (which are assumed to be the band- and interband-concentrations of C). The usual form of this functional is the Landau–Ginzburg free energy with a functional derivative of the following form

$$\frac{\delta f(c)}{\delta c} = u_0(c - \bar{c}) + v_0(c - \bar{c})^3 + w_0 \Delta c \tag{4}$$

where u_0, v_0, and $\bar{c}$ are phenomenological parameters chosen so that the minima of $f(c)$ are at c_1 and c_h, while w_0 governs the scale for the width of the interface between the regions of c_1 and c_h. The values of these parameters are not known (note that since the values of c_1 and c_h, and the width of the interface regions are not measured, the values of u_0, v_0, and w_0 are not fixed in the given experiment).

According to the experiments, the outer- (inner-) electrolytes of concentrations a_0 (b_0) are initially homogeneously distributed inside (outside) of a circle of radius R. Thus, denoting the radial coordinate by r, the initial conditions to Eqs. (1)–(3) are as follows

$$a(r, t = 0) = a_0 \theta(R - r), \quad b(r, t = 0)$$
$$= b_0 \theta(r - R), \quad c(r, t = 0) = 0 \tag{5}$$

where $\theta(x)$ is the step function. The radial symmetry is not broken during the evolution of the precipitation pattern and, consequently, we can limit the solution of Eqs. (1)–(3) to radially symmetric concentration fields $a(r, t)$, $b(r, t)$, and $c(r, t)$. The reduction to a one-dimensional problem greatly simplifies the numerical solution of the equations and even a simple Euler scheme is sufficiently fast and stable to obtain the time evolution of the system.

The difficulty lies in the number of phenomenological parameters. Setting the concentration scale and the length-scale by a_0 and R, respectively, using a timescale which yields $D_A = 1$, and making a further simplification by assuming $D_B = D_A$, one still has five parameters ($u = \lambda u_0$, $v = \lambda v_0$, $w = \lambda w_0$, k, g). The values of these parameters are not known and they can change by several

orders of magnitudes in various systems. Thus, one faces the problem of searching for agreement with the experiment in a five-dimensional parameter space. This is a highly nontrivial problem, and we began by restricting our search to qualitative solutions explaining the most interesting part of the experiment, namely the reversal of the motion of front and the generation of stationary bands in the wake of it. Fig. 4 shows the details of dynamics of the reversal and the formation of multiple bands. As the outer electrolyte A is depleted, the reaction front stops and, as a result, the outer edge of the precipitate ceases moving ($t = 100$–150). Then, due to dissolution, the outer edge starts to move backward ($t = 150$–200) and the band becomes narrower. As the reaction front reverses its motion, the precipitation takes place behind the outer edge ($t = 200$–240). During this stage, a complicated interplay of reaction–precipitation–dissolution yields a double peak band structure. As the reaction front moves in further, the inner edge of the band starts to move in as well ($t = 240$–250). Now, the concentration of A is still large

enough behind the front to dissolve part of the band, and a band-splitting takes place ($t = 250$). As the front moves in further, the inner band follows it and the A's are so much depleted in the wake of the front that they are not able to dissolve the outer band ($t = 250$–300). From this point on, the process is similar to usual Liesegang band formation [17]: the reaction product of the moving front phase separates in the wake of the front, and the bands formed in this way are stable since the dissolution is negligible due to the depletion of the A's ($t = 300$–350). The band formation stops once the concentration of the reaction product in the front decreases below a threshold set by the Cahn–Hilliard equation.

Once qualitative agreement is found, a quantitative comparison with the experiments may also be attempted. E.g. the time-evolution of the radius $r_f(t)$ and width $w(t)$ of the pulse can be calculated and measured in detail. We did this in a regime where the concentrations of a_0 and b_0 are chosen such that the front just driven out, then stops, and no reverse motion takes place. Fig. 5a shows a set of
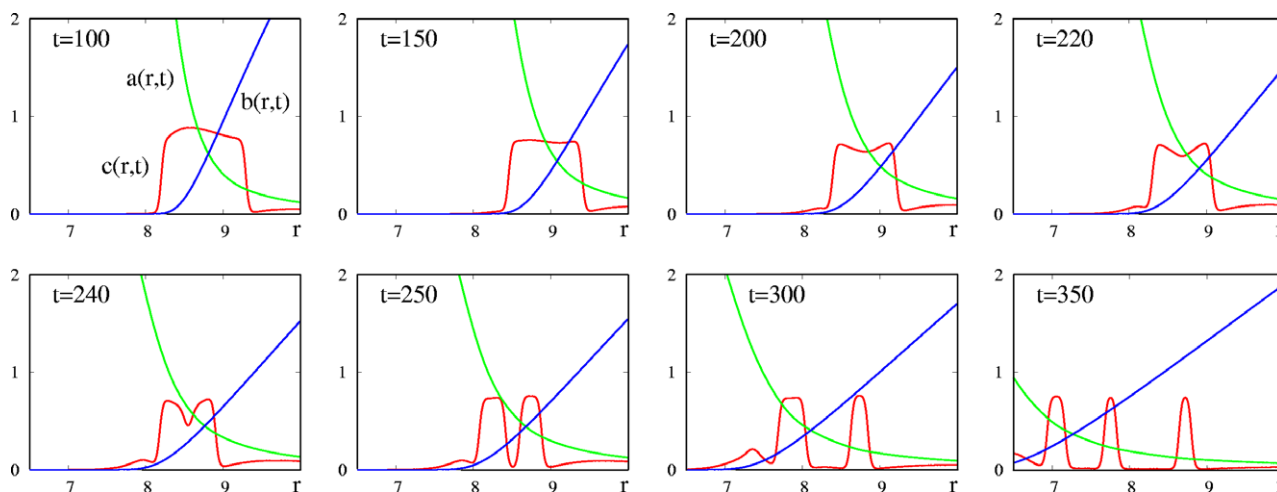

Fig. 4. Formation of multiple bands after reversal of the reaction front. First panel shows the line-assignment to the outer (B) and inner (A) electrolytes, and to the precipitate (C). Detailed explanation of the process can be found in the text. The above figures are obtained by solving Eqs. (1)–(3) using the following parameters: $a_0 = 25$, $b_0 = 0.4$, $u = 0.15$, $v = 550$, $w = 1$, $k = 4$, $g = 0.005$, and $R = 350$.
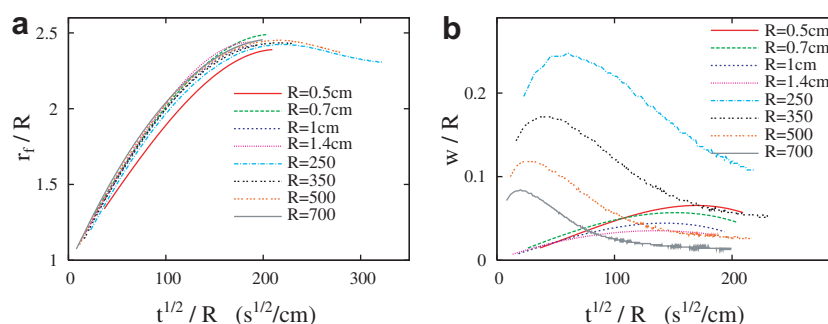

Fig. 5. Time evolution of the radius (a) and the width (b) of the pulse scaled by the radius of the initial interface (R). The time is scaled by R^2. Both experimental (R) and theoretical (R) results are shown with the scales on the horizontal axis related through $(t^{1/2}/R)_{exp} = 5.7 \times 10^3 (t^{1/2}/R)_{th}$. The parameters used in the numerical solution of Eqs. (1)–(3) were $a_0 = 25$, $b_0 = 0.4$, $u = 0.4$, $v = 100$, $w = 1$, $k = 0.3$ and $g = 0.002$.

Table 1
Experimentally observed relationship between the radius R of the initial interface between the reagents and the radius $r_f(\infty)$ of the final position of the precipitation ring ($[AlCl_3]_0 = 0.04$ M)

R (mm)	5	7	10	14
$r_f(\infty)/R$	2.44 ± 0.07	2.52 ± 0.05	2.45 ± 0.03	2.46 ± 0.02

experimental and theoretical results for time evolution of the front position, $r_f(t)$ scaled by the radius of the initial interface (R). The scaling by R is suggested by calculating the final position of the front [$r_f(\infty)$] by finding the radius of area where the B's are in sufficient number to consume all the A's. This calculation suggests that $r_f(\infty)/R$ is constant, independent of R. As can be seen from Table 1, the relationship $r_f(\infty)/R =$ constant is indeed satisfied.

In Fig. 5a, the radius of the pulse is plotted against $t^{1/2}/R$ and good collapse is found for both experimental and theoretical curves for various R's. This shows that although the front motion is not simply diffusive, the front dynamics has the scale-invariance of diffusive processes, and the theoretical model captures this aspect correctly. Note that the agreement between the experiment and theory is also excellent. The collapse is achieved for the experimental ratio of initial concentrations ($b_0/a_0 = 0.016$) by finding an appropriate set of reaction rates and Landau coefficients, and using a scale factor to relate the experimental and theoretical timescales (see caption of Fig. 5).

Problems arise in the quantitative description of the width of the precipitation zone. As can be seen in Fig. 5b, the agreement between theory and experiment is at most qualitative. While both widths grow initially and then show a decreasing trend, there are important differences. The theoretical widths are significantly larger and, furthermore, they reach their maxima well before the band stops ($t^{1/2}/R \approx 200$, see Fig. 5a). This is in contrast to the experimental widths which increase almost to the end of the band motion. The narrower experimental widths may be explained by the uncertainties of what is measured in the experiment as compared to the theory. The shift of the maxima, however, is harder to explain. The underlying reason may be the simplicity of the Landau free energy where the u_0 and v_0 set a constant concentration of C in the band. Visual observations, however, indicate that the structure of the band and thus the concentration in them is changing during the evolution. Consequently, u_0 and v_0, and perhaps λ and w_0 as well, are functions of the local concentration of A.

The a-dependence of the free energy is an interesting problem and the solution may also be relevant for building a more powerful theory of Liesegang phenomena [19,20]. Indeed, the explanation of the so-called width-law of Liesegang phenomena is based on phase-separation scenario with an underlying free energy. A consequence of this theory is the constancy of the precipitate concentration in the bands which is not always seen in experiments [21]. A natural explanation is again in the generalization of the free energy. At this point, however, one would need more experimental input to build a more complicated model. This is outside the scope of this Letter.

4. Final remarks

We have investigated a precipitation process where limited feeding of the invading electrolyte, precipitation, and a complex-formation process combine to yield a precipitation pulse with nontrivial motion and with the possibility of evolution into a multi-band structure. An explanation for the various phenomena can be found through the reaction front dynamics governed by the direction of the higher transport flux of electrolytes. In contrast to classical setups where the high initial concentration of the outer electrolyte ensures its dominant flux into inner electrolyte, the limited feeding of the external electrolyte produces a reaction-front reversal. As a consequence, a Liesegang type band-formation is developed in direction of the source of the external electrolyte. Presumably, this type of reaction-front reversals underlie the explanation of several seemingly revert Liesegang structures in chemistry and geoscience. The experimental results have been described using a phase separation scenario for the precipitation formation and adding the process of redissolution through complex formation. The model captures all important features and, we believe, it may be the basis for understanding rather complex Liesegang type precipitation patterns.

Acknowledgements

References

[1] R.E. Liesegang, Naturwiss. Wochenschr. 11 (1896) 353.
[2] O. Giraldo, Nature 405 (2000) 38.
[3] M.I. Lebedeva, D.G. Vlachos, M. Tsapatsis, Phys. Rev. Lett. 92 (2004) 088301.
[4] M.I. Lebedeva, D.G. Vlachos, M. Tsapatsis, Ind. Eng. Chem. Res. 43 (2004) 3073.
[5] M. Fialkowski, A. Bitner, B.A. Grzybowski, Phys. Rev. Lett. 94 (2005) 018303.
[6] B.A. Grzybowski, K.J.M. Bishop, C.J. Campbell, M. Fialkowski, S.K. Smoukov, Soft Matter 1 (2005) 114.
[7] M. Zrínyi, L. Gálfi, É Smidróczki, Z. Rácz, F. Horkay, J. Phys. Chem. 95 (1991) 1618.
[8] I. Das, A. Pushkarna, N.R. Agrawal, J. Phys. Chem. 93 (1989) 7269.
[9] I. Das, A. Pushkarna, A. Bhattacharjee, J. Phys. Chem. 95 (1991) 3866.
[10] R. Sultan, S. Sadek, J. Phys. Chem. 100 (1996) 16912.
[11] I. Das, P. Singh, N.R. Agrawal, R.P. Rastogi, J. Colloid Interf. Sci. 192 (1997) 420.

[12] R.F. Sultan, Phys. Chem. Chem. Phys. 4 (2002) 1253.

[13] I. Lagzi, J. Phys. Chem. B 107 (2003) 13750.

[14] A. Volford, F. Izsák, M. Ripszám, I. Lagzi, J. Phys. Chem. B 110 (2006) 4535.

[15] J. George, G. Varghese, J. Mater. Sci. 40 (2005) 5557.

[16] H. Taitelbaum, Y-E.L. Koo, S. Havlin, R. Kopelman, G.H. Weiss, Phys. Rev. A 46 (1992) 2151.

[17] T. Antal, M. Droz, J. Magnin, Z. Rácz, Phys. Rev. Lett. 83 (1999) 2880.

[18] T. Antal, M. Droz, J. Magnin, A. Pekalski, Z. Rácz, J. Chem. Phys. 114 (2001) 3770.

[19] M. Droz, J. Magnin, M. Zrínyi, J. Chem. Phys. 110 (1999) 9618.

[20] Z. Rácz, Physica A 274 (1999) 50.

[21] M. Zrínyi, unpublished.